

# Thy1 Associates with the Cation Channel Subunit HCN4 in Adult Rat Retina

Gloria J. Partida,<sup>1</sup> Tyler W. Stradleigh,<sup>1</sup> Genki Ogata,<sup>1</sup> Iv Godzdanker,<sup>1</sup> and Andrew T. Ishida<sup>1,2</sup>

**PURPOSE.** The membrane expression and gene promoter of the glycosylphosphatidylinositol (GPI)-anchored protein Thy1 have been widely used to examine the morphology and distribution of retinal ganglion cells in normal eyes and disease models. However, it is not known how adult mammalian retinal neurons use Thy1. Because Thy1 is not a membrane-spanning protein and, instead, complexes with structural and signaling proteins in other tissues, the aim of this study was to find protein partners of retinal Thy1.

**METHODS.** Coimmunoprecipitation, immunohistochemistry, confocal imaging, and patch-clamp recording were used to test for association of Thy1 and HCN4, a cation channel subunit, in adult rat retina.

**RESULTS.** Hyperpolarization of cells immunopanned by an anti-Thy1 antibody activated HCN channels. Confocal imaging showed that individual somata in the ganglion cell layer bound antibodies against Thy1 and HCN4, that the majority of these bindings colocalized, and that some of the immunopositive cells also bound antibody against a ganglion cell marker (Brn3a). Consistent with these results, Thy1 and HCN4 were coimmunoprecipitated by magnetic beads coated with either anti-Thy1 antibody or anti-HCN4 antibody. In control experiments, beads coated with these antibodies did not immunoprecipitate a photoreceptor rim protein (ABCR) and uncoated beads did not immunoprecipitate either Thy1 or HCN4.

**CONCLUSIONS.** This is the first report that Thy1 colocalizes and coimmunoprecipitates with a membrane-spanning protein in retina, that Thy1 complexes with an ion channel protein in any tissue, and that a GPI-anchored protein associates with an HCN channel subunit protein. (*Invest Ophthalmol Vis Sci.* 2012;53:1696-1703) DOI:10.1167/iovs.11-9307

From the <sup>1</sup>Section of Neurobiology, Physiology, and Behavior and the <sup>2</sup>Department of Ophthalmology and Vision Science, University of California, Davis, California.

Supported by National Institutes of Health Grant EY08120, NIH American Recovery and Reinvestment Act Award (EY08120-20S1), a National Eye Institute Core grant (P30 EY12576), a Research Award from the Plum Foundation, and a Departmental grant to the Department of Ophthalmology from Research to Prevent Blindness, Inc., New York, New York. T.W.S. was supported at different phases of this work by an NIH Research Supplement to Promote Diversity in Health-Related Research (EY08120-17S1), an NIH-NEI Training Grant (T32 EY015387), and an NIH-IMSD Fellowship (R25 56765).

Submitted for publication December 15, 2011; accepted January 15, 2012.

Disclosure: **G.J. Partida**, None; **T.W. Stradleigh**, None; **G. Ogata**, None; **I. Godzdanker**, None; **A.T. Ishida**, None

Corresponding author: Andrew T. Ishida, Department of Neurobiology, Physiology, and Behavior, University of California, One Shields Avenue, Davis, CA 95616-8519; atishida@ucdavis.edu.

Neuronal cell membranes are populated by topologically diverse proteins. Some of these proteins contain membrane-spanning domains and expose amino acid sequences to the extra- and intracellular milieus. These include the large variety of ion channels and neurotransmitter receptors which enable neurons to generate, regulate, and transmit electrical signals. Other proteins lodge in the outer leaflet of cell membranes, lack membrane-spanning domains, and contribute to cellular functions by coordinating with nearby membrane-spanning proteins and/or with proteins penetrating the inner membrane leaflet from the intracellular side. The outer leaflet proteins include adhesion molecules, growth-associated proteins, and signal transduction molecules anchored to membranes by covalent linkage to glycosylphosphatidylinositol (GPI; e.g., CPG15, GFR, contactin, kilon, NgR, PrP<sup>C</sup>).<sup>1-6</sup> The prototypical glycoprotein of this class is Thy1 (also known as CD90). It was the first vertebrate GPI-anchored protein to be discovered, it is found in several regions of the central nervous system, and it has been used as a marker in cell identification, immunopanning, retrieval, monitoring, and targeting strategies.<sup>7-15</sup>

In adult retina, Thy1 localizes largely to a single class of neuron (retinal ganglion cells).<sup>16,17</sup> Numerous studies have leveraged this to visualize the shape and distribution of cells in normal retina, and to achieve single-cell resolution in large-scale searches for changes and losses of cells in disease models.<sup>18-24</sup> Although the presence of Thy1 in adult retinal ganglion cells has been known for three decades,<sup>25</sup> and although Thy1 associates with a wide variety of proteins during cellular interactions and signaling events in other tissues (e.g., 4.1, Src kinase, Gai,  $\beta$ 3 integrins),<sup>26-29</sup> previous studies have not identified any protein that affiliates with Thy1 in the normal, adult retina of any species. Here, we test the possibility that Thy1 links with an integral membrane protein contributing to resting potential, input resistance, and rebound excitation in adult rat retinal ganglion cells<sup>30,31</sup> and present biochemical, immunohistochemical, and electrophysiological evidence that Thy1 associates and colocalizes with the ion channel subunit protein known as HCN4.<sup>32</sup>

## MATERIALS AND METHODS

### Animals

Adult rat retinas were used for the experiments reported here because anti-Thy1 and anti-HCN4 antibodies bind to neurons in this tissue.<sup>16,31,33-35</sup> Long-Evans rats (female; postnatal day [P]60 to P120; 150 to 250 g) were obtained from a commercial supplier (Harlan Bioproducts; San Diego, CA) and housed in standard cages at approximately 23°C on a 12-hour/12-hour light/dark cycle. Before enucleating eyes for all experiments described here, rats were euthanized by a lethal dose of sodium pentobarbital (150 mg/kg, intraperitoneally). All animal care and experimental protocols were approved by the Animal Use and Care Administrative Advisory Committee of the University of Califor-

nia, Davis, and conducted in accordance with the ARVO Statement for the Use of Animals in Ophthalmic and Vision Research.

### Patch-Clamp

Current flowing through HCN channels ( $I_h$ ) was recorded from adult rat retinal ganglion cell somata using dissociation protocols, cell immunopanning by anti-Thy1 antibody, whole-cell patch electrodes, perforated-patch recording mode, a patch-clamp amplifier (Axopatch 200B; Molecular Devices, Sunnyvale, CA), stimulus generation, pharmacological blockers, data acquisition, whole-cell capacitance measurement by nulling slow capacitive current, and liquid junction potential correction, as described elsewhere.<sup>30,31</sup> These methods enabled us to test for the presence of  $I_h$  in cells immunopanned by antibody of the same clone as we used in the immunohistochemical and immunoprecipitation experiments (see below for a description of the antibodies used in this study). The composition and osmolarity of the patch-electrode and external superfusate solutions are described elsewhere.<sup>31</sup> The pH of the external solution was adjusted to 7.4 by bubbling with carbogen (95% O<sub>2</sub>, 5% CO<sub>2</sub>). Voltage-gated Na<sup>+</sup> and Ca<sup>2+</sup> currents were blocked by tetrodotoxin (1 μM), elevated Mg<sup>2+</sup> (3.4 mM), and lowered Ca<sup>2+</sup> (0.1 mM).<sup>30,31</sup> A few experiments were performed in ruptured-patch mode with an electrode-filling solution containing (in mM) 115 K-D-gluconic acid, 15 KCl, 15 NaOH, 2.6 MgCl<sub>2</sub>, 0.34 CaCl<sub>2</sub>, 1 EGTA, 10 HEPES, 2 ATP, 0.4 GTP, and 3 glutathione (reduced), along with physiological external divalent cation levels (2.5 mM Ca<sup>2+</sup>, 1.5 mM Mg<sup>2+</sup>). Currents were recorded at 35°C.

### Immunohistochemistry

Freshly enucleated eyes were hemisected in an ice cold dissection solution (Sorensen's phosphate buffer; 67 mM, pH 7.4, supplemented with 150 mM sucrose, 1 mM EGTA, 1 mM MgCl<sub>2</sub>) and then fixed in paraformaldehyde (4% in dissection solution) for 60 minutes at room temperature. Fixed retinas were placed vitreous side up on a polycarbonate membrane filter (HTBP01300; Millipore, Billerica, MA) and flattened onto the filter by applying suction to the opposite side. The filter-bound retinas were rinsed in PBS, and quenched for 30 minutes in glycine (1% wt/vol in dissection solution). Retinas were then incubated overnight at 4°C in primary antibody (diluted in PBS supplemented with 5% normal donkey serum; 017-000-121, Jackson ImmunoResearch, West Grove, PA), rinsed with PBS, and incubated overnight in secondary antibody (diluted in PBS). Pairs of primary and secondary antibodies were applied sequentially by incubating in the first primary antibody, the first fluorophore-conjugated secondary, the second primary, and then the second fluorophore-conjugated secondary, with ample PBS rinses in between. In all experiments, the anti-HCN4 antibody was applied first. When staining with two monoclonal primary antibodies, the first secondary antibody was a fluorophore-conjugated anti-mouse Fab fragment. This was followed by a 6-hour application of unconjugated anti-mouse Fab fragments (715-007-003, diluted 1:50; Jackson ImmunoResearch) to minimize the chance of primary antibody cross-reactivity.<sup>31</sup> Some retinas were stained with anti-Brn3a antibody (diluted in the solution containing the anti-Thy1 antibody) to aid in identification of retinal ganglion cells (see Nadal-Nicolás et al.<sup>36</sup>). Other retinas were counterstained for 30 minutes at room temperature with deep-red fluorescent Nissl stain (NeuroTrace, N-21483; Invitrogen, Carlsbad, CA), diluted 1:500 in PBS. After final rinses in PBS, flattened retinas were mounted directly to glass coverslips (number 1.5), covered with mounting medium (Vectashield, H-1000, Vector Laboratories, Burlingame, CA), and secured onto glass slides.

### Confocal Imaging and Analysis

Flat-mounted retinas were confocally imaged (FluoView FV1000 Confocal System [version 1.6; Olympus, Center Valley, PA] interfaced to an inverted microscope [IX-81; Olympus]), using the excitation lasers, objectives, sequential fluorophore excitation, independent fluorescence emission collection, optical section intervals, frame averaging,

and image handling software we have described elsewhere.<sup>31</sup> Colocalization analysis of signals attributed to Thy1 and HCN4 was performed using ImageJ (version 1.43; software developed by Wayne Rasband, National Institutes of Health, Bethesda, MD, available at <http://rsb.info.nih.gov/ij/index.html>) and image-processing software (Photoshop CS4; Adobe Systems, San Jose, CA). In ImageJ, each selected optical section was exported to the image-processing software (Photoshop CS4) as an RGB TIFF image file. Signals attributed to Thy1, HCN4, and Brn3a were represented by the red, green, and blue color channels, respectively. The component red, green, and blue channels were separated and converted to grayscale TIFF image files. Cell membranes of HCN4-immunopositive cells were then selected using the ImageJ selection tool. The degree of overlap between Thy1 immunoreactivity and HCN4 immunoreactivity was calculated using a plug-in for ImageJ (Manders' Coefficients; available at: <http://www.uhnresearch.ca/facilities/wcif/software/>) and expressed as Manders' overlap coefficient, a measure of pixel overlap that is independent of average intensity values.<sup>37</sup>

### Membrane Fraction Protein Isolation

Retinas were isolated in phosphate-buffered saline (PBS; pH 7.4, supplemented with 1 mM phenylmethylsulfonyl fluoride), collected in microcentrifuge tubes, and frozen by dropping into liquid nitrogen. Ten to twenty retinas were homogenized in lysis buffer (0.32 M sucrose, 0.1 M Tris-HCl; pH 7.4). The homogenate was centrifuged at 600g for 10 minutes at 4°C and, to produce a membrane fraction, the supernatant was centrifuged at 45,000g for 40 minutes at 4°C. The final pellet was collected and resuspended in solubilization buffer (50 mM NaF, 10 mM Tris-HCl, 0.5% Brij97, 1 mM ethylenediamine tetra-acetic acid, 0.2 M Na<sub>3</sub>VO<sub>4</sub>; pH 7.4). Total protein concentration was determined using a bicinchoninic acid protein assay kit. Unless otherwise noted, all solutions were ice cold and supplemented with protease inhibitor tablets (Complete Mini, 11836153001; Roche, Indianapolis, IN).

### Immunoprecipitation

Samples of the membrane fraction proteins were diluted to 1 mg/mL in 200 μL of solubilization buffer. A 500-μg aliquot of this protein was incubated on a rocker for 40 minutes at 4°C with 50 to 125 μL of protein G-coated beads (Dynabeads, 100.03D; Invitrogen) that had been bound to antibodies directed against various retinal proteins with or without cross-linking with bis(sulfosuccinimidyl) suberate. Unbound proteins were washed from these beads by multiple rinses in solubilization buffer or in Triton X-100 (1% vol/vol in 200 mM NaCl). Bound proteins were eluted off the beads by boiling in lithium dodecyl sulfate sample buffer for 5 to 10 minutes.

### Western Blot Analysis

Membrane fraction protein (referred to hereafter as "lysate") and immunoprecipitated protein from the same retinal homogenate were loaded onto adjacent lanes of a 4%-12% gradient gel (Bis-Tris, NP0321BOX; Invitrogen), electrophoretically separated in MOPS running buffer at 200 V for 1 hour, and transferred to a polyvinylidene difluoride (PVDF) membrane (162-0174; Bio-Rad, Hercules, CA) at 30 V for 1 hour. Protein standards were run in lanes adjacent to the samples. The PVDF membrane was incubated with primary antibodies on a rocker overnight at 4°C. The membranes were then rinsed with Tris-buffered saline (supplemented with 0.5% Tween-20) and incubated in species-specific secondary antibody conjugated to horseradish peroxidase (HRP) or fluorophores for 1 hour at room temperature. These membranes were either probed with only one antibody, divided into parts that were each probed with different antibodies, or sequentially probed after stripping with 100 mM glycine (pH 3.0). Protein bands were visualized in a digital imager (FluorChem Q; Alpha Innotech, San Leandro, CA) by the fluorophore fluorescence or by ECL detection of the HRP using a substrate (SuperSignal West Pico Chemiluminescent Substrate; Thermo Fisher Scientific, Waltham, MA).

## Primary and Secondary Antibodies

The results reported here were obtained with three monoclonal antibodies and two polyclonal antibodies. One anti-HCN4 antibody was an affinity-purified rabbit polyclonal IgG against a fusion protein of GST and amino acids 119 to 155 of human HCN4 (AB5808; Millipore). The other anti-HCN4 antibody was clone N114/10 (73-150; UC Davis/NIH NeuroMab Facility, Davis, CA), a monoclonal mouse IgG1 raised against a fusion protein of GST and amino acids 1019 to 1108 of rat HCN4. The anti-Thy1 antibody was clone OX7 (MAB1406; Millipore), a mouse IgG1 directed against the rat Thy1 isoform (Thy1.1). The mouse monoclonal anti-ABCR antibody was clone 3F4 (ab77285; Abcam, Cambridge, MA), raised against a bovine rod photoreceptor rim protein.<sup>38</sup> The anti-Brn3a antibody (sc-31984; Santa Cruz Biotechnology; Santa Cruz, CA) was a goat polyclonal directed against a region near the N-terminus of human Brn3a.

These primary antibodies were used with species-specific secondary antibodies. Rabbit primary antibodies were visualized on Western blots with a donkey anti-rabbit IgG conjugated to HRP (NA934V; GE Health Care Life Science, Piscataway, NJ) or with a detection reagent (Clean-Blot IP, 21232; Thermo Fisher Scientific). Mouse primary antibodies were visualized on Western blots with a sheep anti-mouse IgG conjugated to HRP (NA931; GE Health Care Life Science) or with Fc fragment-specific, DyLight 649-conjugated goat anti-mouse IgG (115-495-008; Jackson ImmunoResearch). For immunohistochemical colocalizations, the polyclonal HCN4 was stained with a donkey anti-rabbit IgG conjugated to DyLight 488 (711-485-152; diluted 1:200); the monoclonal HCN4 antibody was stained with donkey anti-mouse Fab fragments conjugated to DyLight 488 (715-487-003; diluted 1:50), and the Thy1 antibody was stained with a donkey anti-mouse IgG conjugated to DyLight 549 (715-505-151; diluted 1:200). The Brn3a antibody was stained with a donkey anti-goat IgG conjugated to DyLight 649 (705-495-147; diluted 1:200). These fluorophores were selected because their excitation and emission wavelengths produced minimal cross-contamination.

## Reagents

The reagents used for the electrophysiological recordings were obtained from Sigma-Aldrich (St. Louis, MO), except for tetrodotoxin (554412; EMD Chemicals, Gibbstown, NJ), CaCl<sub>2</sub> (BDH Laboratory Supplies; Poole, UK), and ZD7288 (1000; Tocris Bioscience, Ellisville, MO). The reagents used for the protein isolations, coimmunoprecipitations, and Western blot analysis were obtained from sources listed elsewhere,<sup>31,35</sup> except that the bicinchoninic acid protein assay kit (23227) and bis(sulfosuccinimidyl) suberate (BS<sup>3</sup>; 21658) were obtained from Thermo Fisher Scientific (Waltham, MA). Sodium pentobarbital (0074-378-05) was obtained from Abbott Laboratories (Abbott Park, IL).

## RESULTS

This study uses electrophysiological, immunohistochemical, and biochemical methods to identify a protein associated with Thy1 in adult rat retina. Patch-clamp recording is used to detect a cation current ( $I_h$ ) activated in cells immunopanned by anti-Thy1.1 antibody. Isoform-specific antibodies and confocal imaging are used to test the possibility that Thy1.1 and a subunit of the channel passing  $I_h$  (HCN4) colocalize in individual cells. Lastly, we use coimmunoprecipitation to test the possibility that Thy1.1 and HCN4 are physically associated.

### $I_h$ in OX7-Immunopanned Cells

Thy1 localizes to layers of the adult mammalian retina containing ganglion cell dendrites, somata, and axons.<sup>16</sup> This might reflect partnering of Thy1 with proteins contributing to passive electrophysiological properties, signaling, and/or light responses. However, voltage-gated Na<sup>+</sup> channels, voltage-gated

Ca<sup>2+</sup> channels, Ca<sup>2+</sup>-activated K<sup>+</sup> channels, and glutamate-gated cation channels in other tissues neither associate with, nor incorporate, Thy1<sup>3,39-41</sup> and none of the leak channels found to date in ganglion cells (e.g., TRAAK, ENaC, Eag1/2)<sup>42-44</sup> are known to associate with GPI-anchored proteins. We therefore tested the possibility that Thy1 associates with a channel activated by hyperpolarization of retinal neurons.

As a first step, we used the OX7 clone of anti-Thy1 antibody to immunopann ganglion cells from a suspension of dissociated adult rat retina (cf., Barres et al.<sup>9</sup>) and used patch-clamp methods to measure whole-cell currents activated by hyperpolarizations from a holding potential of -62 mV to test potentials ranging from -67 to -87 mV. After the onset of each hyperpolarizing step, the clamp current increased in amplitude instantaneously and then continued to increase gradually. During the largest hyperpolarizations (e.g., to -87 mV), this current rose to a peak amplitude within 1 second and remained at that amplitude for the remainder of the test hyperpolarization. After the offset of these hyperpolarizations, the clamp current gradually returned to baseline. Together with the slow kinetics, the inward polarity of the currents at voltages positive to the K<sup>+</sup> equilibrium potential (-96 mV, based on the superfusate and patch electrode K<sup>+</sup> concentrations) suggests that the inward current is  $I_h$ .<sup>30</sup> Consistent with this identification, 3 mM Cs<sup>+</sup> and 100  $\mu$ M ZD7288 abolished the slow current activated by hyperpolarization and the tail current on repolarization<sup>30</sup> (Fig. 1). Fits of the sum of two exponential time functions to the current blocked by ZD7288 ( $n = 3$ ) and to the current blocked by Cs<sup>+</sup> ( $n = 4$ ) yielded similar kinetic time constants (mean  $\pm$  SEM). The former (ZD7288) yielded  $454 \pm 120$  and  $3697 \pm 1022$  msec as the fast and slow activation time constants for steps from -62 to -87 mV, and  $543 \pm 23$  and  $7737 \pm 1956$  msec as fast and slow deactivation time constants for steps from -87 to -62 mV. For the same steps, the latter (Cs<sup>+</sup>) yielded  $458 \pm 110$  and  $3788 \pm 932$  msec as the fast and slow activation time constants, and  $662 \pm 156$  and  $3207 \pm 2433$  msec as fast and slow deactivation time constants.

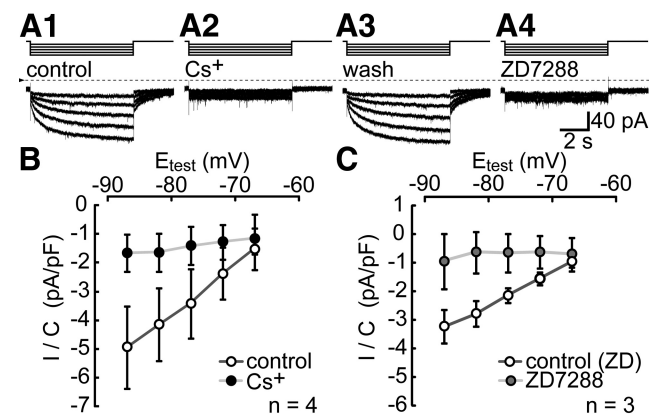


**FIGURE 1.**  $I_h$  in cells immunopanned by anti-Thy1 antibody.  $I_h$  activated in a single cell by hyperpolarizations from the holding potential (-62 mV) to -67, -72, -77, -82, and -87 mV, while the superfusate was changed from control (A1), to 3 mM Cs<sup>+</sup> (A2), to control solution again (A3), and then to 100  $\mu$ M ZD7288 (A4). Steps above the current traces show stimulus timing. The duration of each test hyperpolarization was 7 seconds. The dotted line shows the zero-current level. Records are displayed without leak subtraction. (B) and (C) show the current density (pA/pF) of the tail currents. These were isolated by digitally subtracting the current in Cs<sup>+</sup> or ZD7288 from the control current, measuring the current amplitude at the holding potential at 50 msec after repolarizing from each of the test potentials ( $E_{test}$ ), and dividing by the whole-cell capacitance. Dots plot the mean of values measured in control solution (white), Cs<sup>+</sup> (black), and ZD7288 (gray). Error bars,  $\pm 1$  SEM.  $n = 3$  in (B);  $n = 4$  in (C).

### Thy1 and HCN4 Colocalize in Brn3a-Immunopositive Cells

The ion channels passing  $I_h$  in rat retinal ganglion cells appear to be formed by subunits denoted HCN1 and HCN4.<sup>31</sup> The results in Figure 1 predict that these subunits populate ganglion cell membranes together with Thy1. As shown in Figure 2, we tested this possibility by laser scanning confocal imaging flat-mounted retinas that had been incubated in primary antibodies directed against amino acid sequences of rat HCN4 (<http://www.expasy.ch/sprot/sprot-top.html>), Thy1.1 (the rat isoform of Thy1),<sup>8</sup> Brn3a (a retinal ganglion cell marker),<sup>36</sup> and fluorophore-conjugated secondary antibodies. Figure 3 illustrates the binding pattern obtained with the anti-HCN4 and anti-Thy1 antibodies in Nissl-stained tissue. These experiments were performed with anti-HCN4 antibodies and not anti-HCN1 antibodies because ganglion cells expressing HCN4 also express HCN1,<sup>31</sup> we obtained more intense labeling with anti-HCN4 antibodies,<sup>35</sup> and two of the three available detector channels of our confocal system were used to image Thy1 and either Brn3a or Nissl. Moreover, we did not identify retinal ganglion cells by retrograde labeling<sup>31,35</sup> to avoid any possibility that this alters Thy1 labeling.<sup>23,45,46</sup>

Figure 2 shows a single optical section through the ganglion cell layer of a retina incubated in monoclonal anti-HCN4 primary and DyLight 488-conjugated secondary (Figs. 2A, 2C), anti-Thy1 primary and DyLight 549-conjugated secondary (Figs. 2B, 2C), and anti-Brn3a primary and DyLight 649-conjugated secondary (Fig. 2C). The fluorescence emissions from DyLight 488, 549, and 649 were assigned to the green, red, and blue

color channels, and are merged in Figure 2C. Yellow in Figure 2C shows colocalization of HCN4- and Thy1-like immunoreactivities along the membranes of several somatic profiles. The condensed intracellular blue signal identifies two of these cells (one each at the upper left and far right of the field) as retinal ganglion cells. Colocalization of Thy1 and HCN4 in single retinal ganglion cells is thus shown by the green and red pixels circumscribing the optically sectioned profile of cells with blue pixels in their nuclei. Figures 2A–C also show HCN4- and Thy1-like immunoreactivities in a nerve fiber layer fascicle (upper right), and one large soma (along the lower edge of the field) without detectable Brn3a-like immunoreactivity. These stainings are compatible with previous descriptions of HCN4-immunopositive, dextran-backfilled somata, and intraretinal nerve fiber bundles.<sup>35</sup> Figures 2D–F show a single optical section through the ganglion cell layer of a different portion of the same retina, processed as in Figures 2A–C except that the anti-Thy1 primary was not applied. The lack of DyLight 549-fluorescence in Figures 2E and 2F show that the colocalization in Figure 2C is not due to binding of both secondary antibodies to the anti-HCN4 primary. Some of the somatic profiles in Figures 2C and 2F bind both anti-Brn3a and anti-HCN4 antibodies, while a few present HCN4-like immunoreactivity without Brn3a-like immunoreactivity (consistent with the results of Oi et al.<sup>35</sup>). Results similar to those illustrated in Figure 2 were obtained in a total of four separately processed retinas.

To demonstrate isoform-specificity of the labeling by anti-HCN4 antibody, we used a polyclonal antibody directed against a different amino acid sequence than the monoclonal antibody.

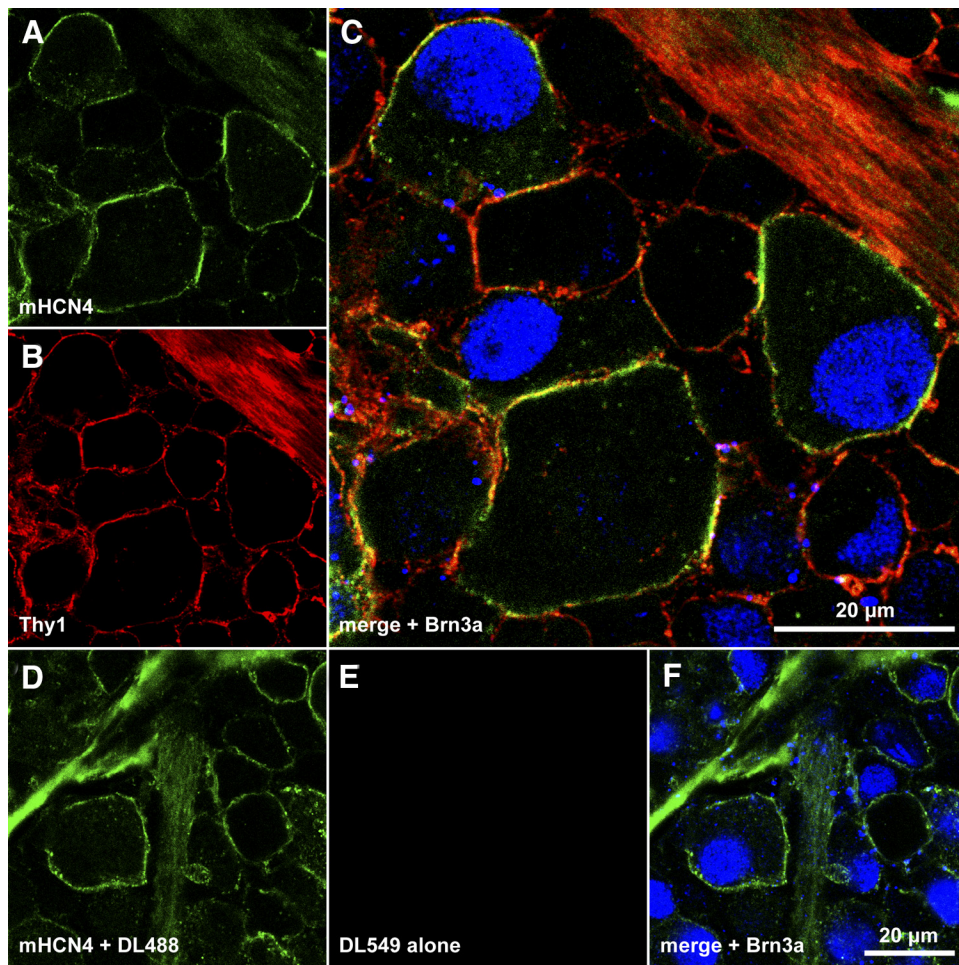


**FIGURE 2.** Colocalization of Thy1 and HCN4 in ganglion cell somata. (A–C) A single optical section through the ganglion cell layer of a retina incubated in monoclonal anti-HCN4 primary and DyLight 488-conjugated secondary (A, C), anti-Thy1 primary and DyLight 549-conjugated secondary (B, C), and anti-Brn3a primary and DyLight 649-conjugated secondary (C). Fluorescence from DyLight 488, 549, and 649 were assigned to the *green*, *red*, and *blue* color channels, respectively, and are merged in (C). (D–F) Single optical section through the ganglion cell layer of a different portion of the same retina, processed as in (A–C) except that the anti-Thy1 primary was not applied. The *scale bar* in (C) (20  $\mu$ m) applies to (C) alone; the *scale bar* in (F) (20  $\mu$ m) applies to (A, B, D–F).

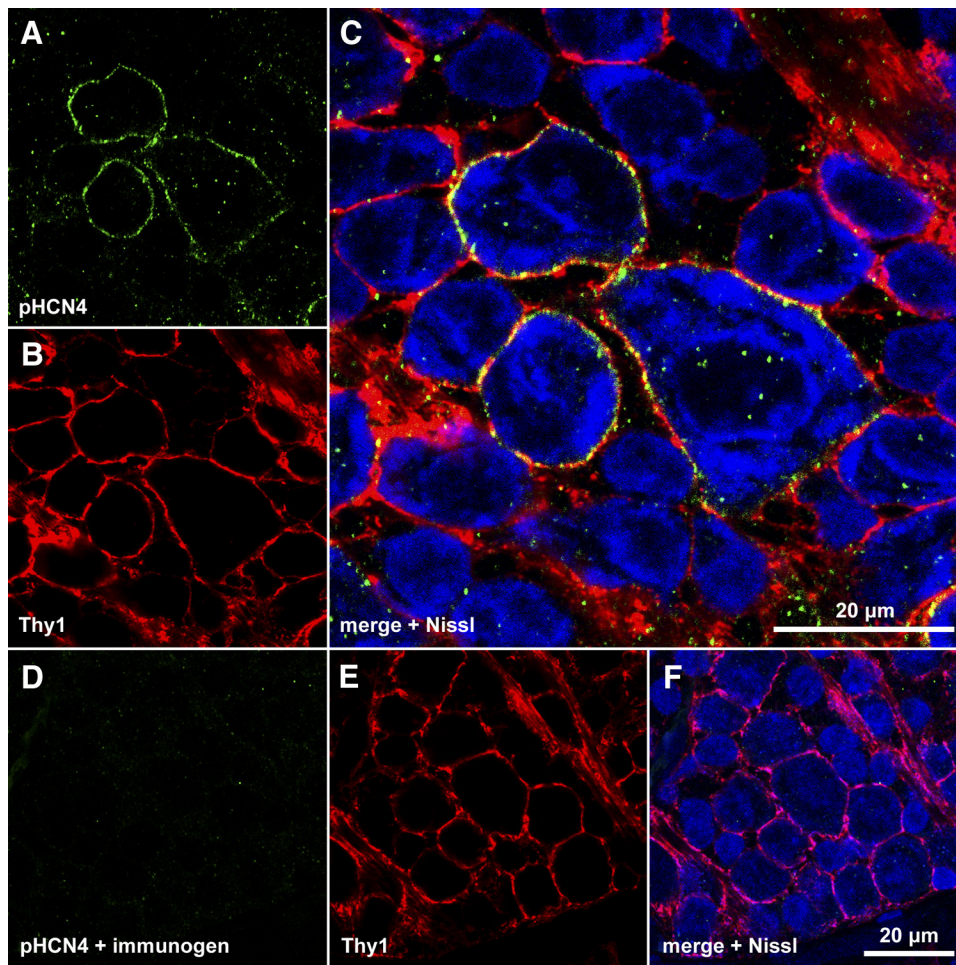


**FIGURE 3.** Colocalization of Thy1 and HCN4 in ganglion cell layer somata. (A–C) Single optical section through the ganglion cell layer of a retina incubated in polyclonal anti-HCN4 primary and DyLight 488-conjugated secondary, anti-Thy1 primary, and DyLight 549-conjugated secondary, and Nissl stain. Fluorescence from DyLight 488 (A), DyLight 549 (B), and Nissl (C) assigned to the green, red, and blue color channels, respectively, and merged in (C). (D–F) Single optical section through the ganglion cell layer of a different portion of the same retina, processed as in (A–C) except that the anti-HCN4 primary was preincubated with immunogen. The scale bar in (C) (20  $\mu\text{m}$ ) applies to (C) alone; the scale bar in (F) (20  $\mu\text{m}$ ) applies to (A, B, D–F).

Figure 3 shows a single optical section through the ganglion cell layer of a retina incubated in polyclonal anti-HCN4 primary and DyLight 488-conjugated secondary, anti-Thy1 primary and DyLight 549-conjugated secondary, and Nissl stain. Fluorescence emissions from DyLight 488 (Fig. 3A), DyLight 549 (Fig. 3B), and Nissl (Fig. 3C) were assigned to the green, red, and blue color channels, respectively, and are merged in Figure 3C. Yellow in Figure 3C shows colocalization of HCN4- and Thy1-like immunoreactivities along the membranes of somatic profiles. The blue signal is cytoplasmic (rather than nuclear as in Fig. 2) and does not distinguish ganglion and displaced amacrine cells.<sup>47</sup> A few medium and small profiles are Nissl-stained but show neither Thy1- nor HCN4-like immunoreactivity. Figures 3D–F show a single optical section through the ganglion cell layer of a different portion of the same retina, processed as in Figures 3A–C except that the anti-HCN4 primary was preincubated with immunogen. The lack of DyLight 488-fluorescence in Figures 3D and 3F show that the colocalization in Figure 3C is not due to binding of both secondary antibodies to the anti-Thy1 primary, and that the HCN4-like immunoreactivity in Thy1-expressing cells is isoform-specific. Results similar to those illustrated in Figure 3 were obtained in a total of three separately processed retinas.

To assess the degree of colocalization between Thy1 and HCN4, we calculated the Manders' overlap coefficient (MOC) for pixels on the membrane profile of several cells.<sup>31,37</sup> Signals attributed to Thy1 and HCN4 overlapped in 68% of the pixels in cells stained with the polyclonal HCN4 antibody ( $n = 34$ ). Similarly, signals attributed to Thy1 and HCN4 overlapped in 73% of the pixels in cells stained with the monoclonal HCN4

antibody ( $n = 94$ ). The MOC calculated for Brn3a-immunopositive cells (73%,  $n = 35$ ) was indistinguishable from that for Brn3a-immunonegative cells (72%,  $n = 59$ ).

### Thy1 and HCN4 Coimmunoprecipitate

The results illustrated in Figures 1–3 raise the possibility that Thy1 resides in membranes within close proximity of HCN channels. The simplest way to achieve this (especially at low protein densities per unit area of membrane) would be to physically link Thy1 and HCN channels. To test whether Thy1 associates with HCN4, we incubated retinal membrane fraction proteins ("lysate") with magnetic beads coated either with anti-Thy1 antibody or with anti-HCN4 antibody, used SDS-PAGE to separate the proteins eluted from these beads, and probed Western blots of these proteins for Thy1 and HCN4. Controls against nonspecific signals were performed with antibody against the rod outer segment rim protein known as ABCR<sup>38</sup> and with uncoated beads. Also, because the antibody used for immunoprecipitation binds some of the secondary antibody used to detect Thy1 in Western blots, Thy1 antibody was BS<sup>3</sup> cross-linked to the beads in a few experiments, and the strength of this binding was tested by probing blots for Thy1 in the absence of retinal proteins.

Based on standard curves constructed from the distances migrated by protein standards in adjacent lanes, the apparent molecular weight (mean  $\pm$  SEM) of the lysate proteins that bound to the HCN4, Thy1, and ABCR antibodies were estimated to be  $140 \pm 2$  kD ( $n = 9$ ),  $28 \pm 1$  kD ( $n = 10$ ), and  $221 \pm 0.4$  kD ( $n = 5$ ), respectively. The apparent molecular

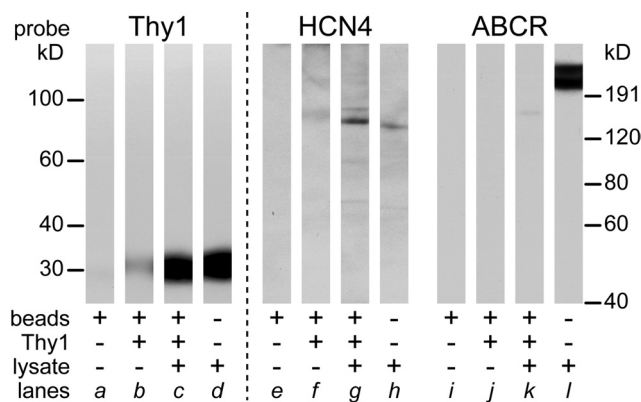


**FIGURE 4.** Coimmunoprecipitation of Thy1 and HCN4 by beads coated with anti-Thy1 antibody. Protein G-coated beads (Dynabeads, 100.03D; Invitrogen) were BS<sup>3</sup>-cross-linked to Thy-1 antibody and then incubated with lysate. Proteins were eluted from these beads, analyzed with Western blot, and sequentially probed for Thy1 (lanes a-d), HCN4 (lanes e-h) using polyclonal antibody, and ABCR (lanes i-l). Before the second and third probes, the previously applied primary antibodies were stripped with glycine. The material aliquoted into each SDS-PAGE gel lane is specified underneath by the combination of + and -. Lanes a, e, and i are material eluted from raw beads (without antibody coating and without lysate). Lanes b, f, and j are material eluted from antibody-coated beads without lysate. Lanes c, g, and k are proteins eluted from Thy1 antibody-coated beads incubated with lysate. Lanes d, h, and l are lysate alone. The migration distances of the molecular weight standards along the left apply to the lanes probed by Thy1 antibody. Those along the right apply to the lanes probed by HCN4 and ABCR antibodies.

weight of the proteins that eluted from beads coated by HCN4 and Thy1 antibodies, and were then detected on Western blots by HCN4 and Thy1 antibodies ( $141 \pm 2$  kD,  $n = 14$ ; and  $28 \pm 1$  kD,  $n = 10$ , respectively), were indistinguishable from those of the lysate proteins (e.g., Figs. 4, 5). These values altogether agree with molecular weight estimates reported previously for these proteins in tissue homogenates (HCN4,<sup>34,35</sup> Thy1,<sup>48</sup> ABCR<sup>36</sup>). For brevity, these bands are referred to below as HCN4, Thy1, and ABCR.

Figure 4 shows that, when incubated with lysate, Thy1 antibody-coated beads coimmunoprecipitated Thy1 and HCN4, and did not immunoprecipitate ABCR (Fig. 4, lanes c, g, k). The other lanes in Figure 4 show that the lysate contained Thy1, HCN4, and ABCR (Fig. 4, lanes d, h, l), that beads without a Thy1 antibody-coating did not release detectable amounts of any material that bound to the Thy1, HCN4, or ABCR antibodies (Fig. 4, lanes a, e, i), and that Thy1 antibody-coated beads (in the absence of lysate) did not release detectable amounts of material that bound to the HCN4 or ABCR antibodies (Fig. 4, lanes f, j). The faint Thy1 signal seen with these beads (Fig. 4, lane b) is consistent with the possibility that a small amount of anti-Thy1 antibody eluted off the beads in this experiment. Results similar to these were obtained with lysate from 5 different batches of rats.

Figure 5 shows that HCN4 antibody-coated beads also coimmunoprecipitated Thy1 and HCN4. The right lane shows that ABCR, HCN4, and Thy1 were present in the lysates (although the HCN4 antibody also bound to protein at 80 kD in this figure, we found this infrequently and also with immunogen-blocked antibody, suggesting that it is nonspecific [cf. Müller et al.,<sup>34</sup>; Oi et al.<sup>35</sup>]). The middle lane in Figure 5 shows that HCN4 antibody-coated beads coimmunoprecipitated Thy1 and HCN4, but not ABCR. Consistent with this result, and with the ability of Thy1 antibody-coated beads to coimmunoprecipitate HCN4 but not ABCR (Fig. 4), the left lane in Figure 5 shows that no detectable amounts of ABCR, HCN4, or Thy1 bound to

uncoated beads. Results similar to those in Figure 5 were obtained in a total of five Western blot analyses of the lysate proteins collected from three batches of rats.

**DISCUSSION**

The observations of the present study provide the first evidence that Thy1 complexes with an ion channel protein, that retinal Thy1 partners with a membrane-spanning protein, and that a GPI-anchored protein associates with an HCN channel subunit protein. Especially because these pairings have not previously been reported, it is natural to ask how Thy1 might contribute to the function of HCN channels, and how HCN4-expressing retinal neurons might function under conditions that alter Thy1 levels.

A variety of possibilities are suggested by biochemical and electrophysiological studies of native and heterologously expressed ion channels in other preparations. For example, the release of Thy1 from lipid rafts by methyl- $\beta$ -cyclodextrin (MBCD),<sup>49</sup> and the effects of MBCD on  $I_h$  of heterologously expressed HCN4 channels<sup>50</sup> suggest that combination with Thy1 and its lipid microenvironment might modulate the biophysical properties of  $I_h$ . Specifically, the MBCD effects reported to date suggest that this association should decrease the amount of  $I_h$  activated by moderate hyperpolarizations by shifting the activation range to more negative voltages, slightly slowing activation, and significantly accelerating deactivation.

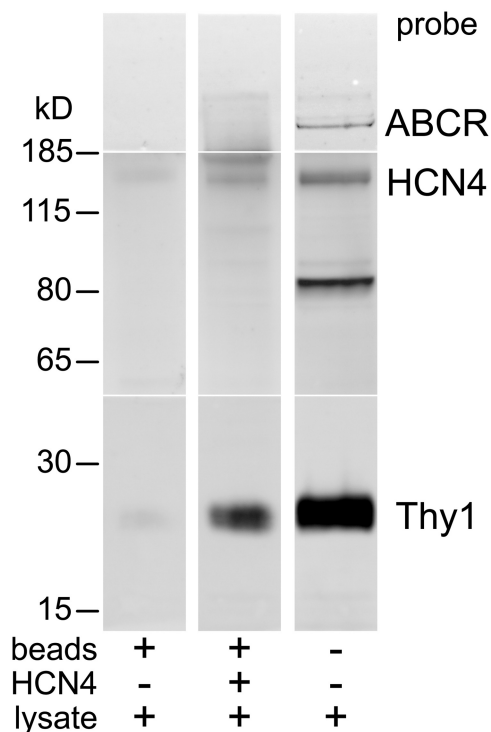


**FIGURE 5.** Coimmunoprecipitation of Thy1 and HCN4 by incubation of beads, coated with monoclonal anti-HCN4 antibody, with lysates, formatted as in Figure 4. The proteins eluted from these beads were separated by SDS-PAGE, with samples of the lysate and molecular weight standards in adjacent lanes. The gels were analyzed with Western blot and the blots were separated into three segments by slicing at the level of the 185 kD standard and at approximately 50 kD. The upper, middle, and lower segments were probed with antibodies against ABCR, HCN4 (polyclonal), and Thy1, respectively. The ABCR and Thy1 antibodies were visualized with Fc fragment-specific, DyLight 649-conjugated, goat anti-mouse IgG. The HCN4 antibody was visualized with detection reagent (Clean-Blot IP; Thermo Scientific).

Secondly, Thy1 could modulate the voltage sensitivity and kinetics of  $I_h$  by decreasing the cAMP sensitivity of retinal HCN channels as in cyclic nucleotide-gated channels.<sup>51</sup> Thirdly, Thy1 might increase, rather than decrease,  $I_h$  in retinal neurons. Although opposite from the expectation laid out above, this would be in concert with effects of other GPI-anchored proteins on other whole-cell currents, including the augmentation of  $Ca^{2+}$ -activated  $K^+$  current by PrP<sup>c</sup>,<sup>39</sup> voltage-gated  $Ca^{2+}$  currents by  $\alpha 2\delta$  subunits,<sup>41</sup> and voltage-gated  $Na^+$  current by *pigu*-dependent anchored proteins.<sup>52</sup>

The interaction of Thy1 and HCN4 is likely to be complicated in at least two respects. One is that Thy1 might interact with retinal HCN channels via adapter proteins, signaling intermediates, and cytoplasmic enzymes as it does with other proteins in nonneuronal preparations (e.g., Haeryfar and Hoskin<sup>53</sup>). Moreover, in the most numerous and conspicuous of the Thy1-expressing cells in retina (retinal ganglion cells),<sup>17</sup> the HCN channels appear to be predominantly heteromeric complexes of HCN1 and HCN4 subunits.<sup>31</sup> Given the possibility that heteromeric and homomeric HCN channels coexist in single cells,<sup>31,54</sup> it would be difficult to attribute effects of MBCD entirely to those seen in the heterologously expressed homomeric channels studied to date.

In any event, the association of Thy1 and HCN4 we have found here implies that changes in Thy1 levels will alter the number of Thy1-partnered HCN channels in single cells. In particular, the coimmunoprecipitation of Thy1 and HCN4, the colocalization of Thy1 and HCN4 in Brn3a-immunopositive cells, and the activation of  $I_h$  in OX7-immunopanned cells, altogether raise the possibility that losses of Thy1 will modulate the contribution of  $I_h$  to the electrophysiological properties of adult ganglion cells.<sup>30</sup> Previous studies suggest two specific conditions under which this might occur. One would be on a daily basis if Thy1 membrane expression fluctuates in a circadian rhythm as found in Thy1 mRNA levels.<sup>55</sup> The second would follow optic nerve damage, when Thy1 expression declines.<sup>45,46</sup> Although mouse lines that do not express Thy1 have been developed (e.g., Nosten-Bertrand et al.<sup>56</sup>), it is uncertain whether these would show how Thy1 loss affects HCN current in the species examined here because the mouse ganglion cell layer expresses at least one HCN isoform that has not been found in rat.<sup>34,57</sup> It is not known if HCN4 and HCN1 colocalize and associate in mouse retinal ganglion cells as they do in rat,<sup>31</sup> and retinal development is abnormal in Thy1 knock-out mice.<sup>58</sup>

### Acknowledgments

The authors thank Aldrin V. Gomes for helpful discussions and comments on the manuscript, and James S. Trimmer for helpful discussions.

### References

- Catallops I, Haas K, Cline HT. Postsynaptic CPG15 promotes synaptic maturation and presynaptic axon arbor elaboration in vivo. *Nat Neurosci.* 2000;3:1004–1011.
- Sarma M. GDNF recruits the signaling crew into lipid rafts. *Trends Neurosci.* 2001;24:427–429.
- Falk J, Bonnon C, Girault JA, Faivre-Sarrailh C. F3/contactin, a neuronal cell adhesion molecule implicated in axogenesis and myelination. *Biol Cell.* 2002;94:327–334.
- Maekawa S, Iino S, Miyata S. Molecular characterization of the detergent-insoluble cholesterol-rich membrane microdomain (raft) of the central nervous system. *Biochim Biophys Acta.* 2003;1610:261–270.
- Yiu G, He Z. Glial inhibition of CNS axon regeneration. *Nat Rev Neurosci.* 2006;7:617–627.
- Aguzzi A, Baumann F, Bremer J. The prion's elusive reason for being. *Annu Rev Neurosci.* 2008;31:439–477.
- Barclay AN, Hydén H. Localization of the Thy-1 antigen in rat brain and spinal cord by immunofluorescence. *J Neurochem.* 1978;31:1375–1391.
- Williams AF, Gagnon J. Neuronal cell Thy-1 glycoprotein: homology with immunoglobulin. *Science.* 1982;216:696–703.
- Barres BA, Silverstein BE, Corey DP, Chun LL. Immunological, morphological, and electrophysiological variation among retinal ganglion cells purified by panning. *Neuron.* 1988;1:791–803.
- Davis TL, Wiley RG. Anti-Thy-1 immunotoxin, OX7-saporin, destroys cerebellar Purkinje cells after intraventricular injection in rats. *Brain Res.* 1989;504:216–222.
- Shoge K, Mishima HK, Mukai S, et al. Rat retinal ganglion cells culture enriched with the magnetic cell sorter. *Neurosci Lett.* 1999;259:111–114.
- Wisden W, Cope D, Klausberger T, et al. Ectopic expression of the GABA(A) receptor alpha6 subunit in hippocampal pyramidal neurons produces extrasynaptic receptors and an increased tonic inhibition. *Neuropharmacol.* 2002;43:530–549.
- Levene MJ, Dombeck DA, Kasischke KA, Molloy RP, Webb WW. In vivo multiphoton microscopy of deep brain tissue. *J Neurophysiol.* 2004;91:1908–1912.
- Bannerman PG, Hahn A, Ramirez S, et al. Motor neuron pathology in experimental autoimmune encephalomyelitis: studies in THY1-YFP transgenic mice. *Brain.* 2005;128:1877–1886.
- Kerrison JB, Duh EJ, Yu Y, Otteson DC, Zack DJ. A system for inducible gene expression in retinal ganglion cells. *Invest Ophthalmol Vis Sci.* 2005;46:2932–2939.
- Barnstable CJ, Dräger UC. Thy-1 antigen: a ganglion cell specific marker in rodent retina. *Neurosci.* 1984;11:847–855.
- Raymond ID, Vila A, Huynh UC, Brecha NC. Cyan fluorescent protein expression in ganglion and amacrine cells in a thy1-CFP transgenic mouse retina. *Mol Vis.* 2008;14:1559–1574.
- Feng G, Mellor RH, Bernstein M, et al. Imaging neuronal subsets in transgenic mice expressing multiple spectral variants of GFP. *Neuron.* 2000;28:41–51.
- Gastinger MJ, Kunselman AR, Conboy EE, Bronson SK, Barber AJ. Dendrite remodeling and other abnormalities in the retinal ganglion cells of Ins2 Akita diabetic mice. *Invest Ophthalmol Vis Sci.* 2008;49:2635–2642.
- Mazzoni F, Novelli E, Strettoi E. Retinal ganglion cells survive and maintain normal dendritic morphology in a mouse model of inherited photoreceptor degeneration. *J Neurosci.* 2008;28:14282–14292.
- Murata H, Aihara M, Chen Y-N, Ota T, Numaga J, Araie M. Imaging mouse retinal ganglion cells and their loss in vivo by a fundus camera in the normal and ischemia-reperfusion model. *Invest Ophthalmol Vis Sci.* 2008;49:5546–5552.
- Leung CK, Weinreb RN. Experimental detection of retinal ganglion cell damage in vivo. *Exp Eye Res.* 2009;88:831–836.
- Raymond ID, Pool AL, Vila A, Brecha NC. A Thy1-CFP DBA/2J mouse line with cyan fluorescent protein expression in retinal ganglion cells. *Vis Neurosci.* 2009;26:453–465.
- Kim I-J, Zhang Y, Meister M, Sanes JR. Lamina restriction of retinal ganglion cell dendrites and axons: subtype-specific developmental patterns revealed with transgenic markers. *J Neurosci.* 2010;30:1452–1462.
- Morris RJ, Ritter MA. Association of Thy-1 cell surface differentiation antigen with certain connective tissues in vivo. *Cell Tissue Res.* 1980;206:459–475.
- Bourguignon LY, Suchard SJ, Kalomiris EL. Lymphoma Thy-1 glycoprotein is linked to the cytoskeleton via a 4.1-like protein. *J Cell Biol.* 1986;103:2529–2540.
- Stefanová I, Horejsí V, Ansotegui IJ, Knapp W, Stockinger H. GPI-anchored cell-surface molecules complexed to protein tyrosine kinases. *Science.* 1991;254:1016–1019.
- Henke RC, Seeto GS, Jeffrey PL. Thy-1 and AvGp50 signal transduction complex in the avian nervous system: c-Fyn and G alpha I protein association and activation of signaling pathways. *J Neurosci Res.* 1997;49:655–670.
- Hermosilla T, Muñoz D, Herrera-Molina R, et al. Direct Thy-1/alphaVbeta3 integrin interaction mediates neuron to astrocyte communication. *Biochim Biophys Acta.* 2008;1783:1111–1120.

30. Lee SC, Ishida AT.  $I_h$  without  $K_r$  in adult rat retinal ganglion cells. *J Neurophysiol*. 2007;97:3790-3799.
31. Stradleigh TW, Ogata G, Partida GJ, et al. Colocalization of hyperpolarization-activated, cyclic nucleotide-gated channel subunits in rat retinal ganglion cells. *J Comp Neurol*. 2011;519:2546-2573.
32. Santoro B, Tibbs GR. The HCN gene family: molecular basis of the hyperpolarization-activated pacemaker channels. *Ann N Y Acad Sci*. 1999;868:741-764.
33. Beale R, Osborne NN. Localization of the Thy-1 antigen to the surfaces of rat retinal ganglion cells. *Neurochem Int*. 1982;4:587-595.
34. Müller F, Scholten A, Ivanova E, Haverkamp S, Kremmer E, Kaupp UB. HCN channels are expressed differentially in retinal bipolar cells and concentrated at synaptic terminals. *Eur J Neurosci*. 2003;17:2084-2096.
35. Oi H, Partida GJ, Lee SC, Ishida AT. HCN4-like immunoreactivity in rat retinal ganglion cells. *Vis Neurosci*. 2008;25:95-102.
36. Nadal-Nicolás FM, Jiménez-López M, Sobrado-Calvo P, et al. Brn3a as a marker of retinal ganglion cells: qualitative and quantitative time course studies in naive and optic nerve-injured retinas. *Invest Ophthalmol Vis Sci*. 2009;50:3860-3868.
37. Manders EMM, Verbeek FJ, Aten JA. Measurement of co-localization of objects in dual-colour confocal images. *J Microscopy*. 1993;169:375-382.
38. Illing M, Molday LL, Molday RS. The 220-kDa rim protein of retinal rod outer segments is a member of the ABC transporter superfamily. *J Biol Chem*. 1997;272:10303-10310.
39. Herms JW, Tings T, Dunker S, Kretzschmar HA. Prion protein affects  $Ca^{2+}$ -activated  $K^+$  currents in cerebellar Purkinje cells. *Neurobiol Dis*. 2001;8:324-330.
40. Hering H, Lin CC, Sheng M. Lipid rafts in the maintenance of synapses, dendritic spines, and surface AMPA receptor stability. *J Neurosci*. 2003;23:3262-3271.
41. Davies A, Kadurin I, Alvarez-Laviada A, et al. The alpha2delta subunits of voltage-gated calcium channels form GPI-anchored proteins, a posttranslational modification essential for function. *Proc Natl Acad Sci USA*. 2010;107:1654-1659.
42. Fink M, Lesage F, Duprat F, et al. A neuronal two P domain  $K^+$  channel stimulated by arachidonic acid and polyunsaturated fatty acids. *EMBO J*. 1998;17:3297-3308.
43. Brockway LM, Zhou ZH, Bubien JK, Jovov B, Benos DJ, Keyser KT. Rabbit retinal neurons and glia express a variety of ENaC/DEG subunits. *Am J Physiol*. 2002;283:C126-C134.
44. Jow GM, Jeng CJ. Differential localization of rat Eag1 and Eag2 potassium channels in the retina. *Neurosci Lett*. 2009;431:12-16.
45. Perry VH, Morris RJ, Raisman G. Is Thy-1 expressed only by ganglion cells and their axons in the retina and optic nerve? *J Neurocytol*. 1984;13:809-824.
46. Schlamp CL, Johnson EC, Li Y, Morrison JC, Nickells RW. Changes in Thy1 gene expression associated with damaged retinal ganglion cells. *Mol Vis*. 2001;7:192-201.
47. Perry VH. Evidence for an amacrine cell system in the ganglion cell layer of the rat retina. *Neurosci*. 1981;6:931-944.
48. Campbell DG, Gagnon J, Reid KB, Williams AF. Rat brain Thy-1 glycoprotein. The amino acid sequence, disulphide bonds and an unusual hydrophobic region. *Biochem J*. 1981;195:15-30.
49. Ilangumaran S, Hoessli DC. Effects of cholesterol depletion by cyclodextrin on the sphingolipid microdomains of the plasma membrane. *Biochem J*. 1998;335:433-440.
50. Barbuti A, Gravante B, Riolfo M, Milanese R, Terragni B, DiFrancesco D. Localization of pacemaker channels in lipid rafts regulates channel kinetics. *Circ Res*. 2004;94:1325-1331.
51. Brady JD, Rich TC, Le X, et al. Functional role of lipid raft microdomains in cyclic nucleotide-gated channel activation. *Mol Pharmacol*. 2004;65:503-511.
52. Nakano Y, Fujita M, Ogino K, et al. Biogenesis of GPI-anchored proteins is essential for surface expression of sodium channels in zebrafish Rohon-Beard neurons to respond to mechanosensory stimulation. *Development*. 2010;137:1689-1698.
53. Haeryfar SM, Hoskin DW. Thy-1: more than a mouse pan-T cell marker. *J Immunol*. 2004;173:3581-3588.
54. Whitaker GM, Angoli D, Nazzari H, Shigemoto R, Accili EA. HCN2 and HCN4 isoforms self-assemble and co-assemble with equal preference to form functional pacemaker channels. *J Biol Chem*. 2007;282:22900-22909.
55. Kamphuis W, Cailotto C, Dijk F, Bergen A, Buijs RM. Circadian expression of clock genes and clock-controlled genes in the rat retina. *Biochem Biophys Res Comm*. 2005;330:18-26.
56. Nosten-Bertrand M, Errington ML, Murphy KP, et al. Normal spatial learning despite regional inhibition of LTP in mice lacking Thy-1. *Nature*. 1996;379:826-829.
57. Mataruga A, Kremmer E, Müller F. Type 3a and type 3b OFF cone bipolar cells provide for the alternative rod pathway in the mouse retina. *J Comp Neurol*. 2007;502:1123-1137.
58. Simon PD, McConnell J, Zurakowski D, et al. Thy-1 is critical for normal retinal development. *Dev Brain Res*. 1999;117:219-223.